DOI: 10.1002/anie.201206737

Drug Delivery

Silicon-Nanowire-Based Nanocarriers with Ultrahigh Drug-Loading Capacity for In Vitro and In Vivo Cancer Therapy**

Fei Peng, Yuanyuan Su, Xinpan Wei, Yimei Lu, Yanfeng Zhou, Yiling Zhong, Shuit-Tong Lee, and Yao He**

With rapid advances of nano-biotechnology, the use of nanomaterials as drug carriers for cancer therapy has received intensive attention in recent years.[1] It is well recognized that only a small amount of traditional anticancer drugs (e.g., doxorubicin DOX, a kind of commercial chemotherapy drug for cancer treatment) can penetrate into tumors.[2] Moreover, drug molecules are prone to be eliminated by renal clearance and distributed in non-target tissues, leading to an insufficient drug concentration at the tumor sites, and thus limited therapeutic effectiveness.[2] To increase the concentration of therapeutic anticancer drugs at the target sites, design of effective carriers with high loading capacity of drug is recognized as an efficacious strategy. In recent years, various nanomaterials have been employed for the design of high-performance drug carriers with large drug-loading capacity, taking advantages of such unique properties of nanomaterials such as a large porous or hollow interior, a huge surface-to-volume ratio.[1] For example, the DOX loading capacity of mesoporous silica structure-based nanocarriers reached as high as about 1200 mg g^{-1},[1f,g] which was further improved to 2350 mg g^{-1} for graphene-oxide-based nanocarriers.[1c,d,h] Liu et al. demonstrated that single-walled carbon nanotubes (SWNTs) show an ultrahigh loading capacity of the DOX (about 4000 mg g^{-1}).[1b] However, those advances remain short of demand for cancer therapy, efforts are still required to develop novel nanomaterial-based drug carriers with a higher drug-loading efficiency.

Silicon nanostructures (e.g., nanodots, nanowires, and nanospheres) feature a favorable biocompatibility and low toxicity, excellent electronic/mechanical properties, a surface that can be tailored, improved multifunctionality, as well as compatibility with conventional silicon technology.[3] Moreover, recent studies reveal that silicon nanomaterials are biodegradable and can self-destruct in a mouse model into components that can be renally cleared without evidence of toxicity in vivo. In addition, silicon is a common trace element in humans and a biodegradation product of porous silicon (e.g., orthosilicic acid) naturally found in numerous tissues.[3d] As a result, silicon nanomaterials have been extensively investigated for various biological applications because of the above unique merits.[3] In particular, silicon nanowires (SiNWs) are highly promising for wide-ranging biological applications, including our recent development of SiNW-based bioprobes for tumor imaging and hyperthermia agents for cancer therapy.[4] Of particular interest, recent studies reveal that SiNWs show excellent catalytic performance owing to the high surface-to-volume ratio and large-area porous structures,[5] which also are two significant factors for the enhancement of the drug-loading capacity.[1] Motivated by those salient features, we herein demonstrate the first example of SiNW-based drug nanocarriers for cancer therapy by using SiNWs as novel nanovectors for delivery of anticancer drugs (DOX). Remarkably, SiNWs are shown to feature an ultrahigh drug-loading capacity of 20800 mg g^{-1}, which is about five times larger than the highest value (of about 4000 mg g^{-1}) ever reported for nanomaterial-based carriers.[1] Significantly, in vitro and in vivo experiments further demonstrate that SiNW-based nanocarriers are highly efficacious for cancer therapy.

Free-standing SiNWs with about 100 nm in diameter and about 500 nm in length are first produced through our previously reported HF-assisted etching method (see the scanning electron microscopy images in Figure S1 in the Supporting Information).[6] Free-standing SiNWs at a concentration of 200 μg mL^{-1} are then mixed with DOX of different concentrations (20–640 μg mL^{-1}) in alkaline aqueous solutions (pH 9) under adequate stirring. The mixed solutions are initially turbid because of the poor aqueous dispersibility of the pure SiNWs, but become gradually transparent with prolonged mixing time, as the hydrophilic DOX molecules are increasingly adsorbed on the SiNWs though interactions between the DOX molecules and the porous silicon surface and weak interactions between the DOX molecules (Figure 1a).[5,7] A clear solution of reddish color is finally observed after 12 h of reaction because of a large amount of DOX molecules loaded onto the SiNWs, forming SiNW–DOX complexes. Centrifugation is further carried out to dispose residual DOX molecules that are not loaded on SiNWs. In brief, the as-prepared SiNW–DOX complex is precipitated under centrifugation (14800 rpm, 15 min), while

[*] F. Peng,[+] Dr. Y. Y. Su,[+] X. P. Wei, Y. M. Lu, Y. F. Zhou, Y. L. Zhong, Prof. S. T. Lee, Prof. Y. He
Institute of Functional Nano & Soft Materials (FUNSOM) and Jiangsu Key Laboratory for
Carbon-based Functional Materials & Devices
Soochow University, Suzhou, Jiangsu 215123 (China)
E-mail: apannale@suda.edu.cn
yaohe@suda.edu.cn

[+] These authors contributed equally to this work.

[**] The authors appreciate financial support from the National Basic Research Program of China (973 program, grant numbers 2013CB934400 and 2012CB932400), NSFC (grant numbers 30900338 and 51072126), the Research Grants Council of HKSAR (grant numbers CityU5/CRF/08 and CityU 101608), and a Project Funded by the Priority Academic Program Development of Jiangsu Higher Education Institutions (PAPD).

Supporting information for this article is available on the WWW under http://dx.doi.org/10.1002/anie.201206737.

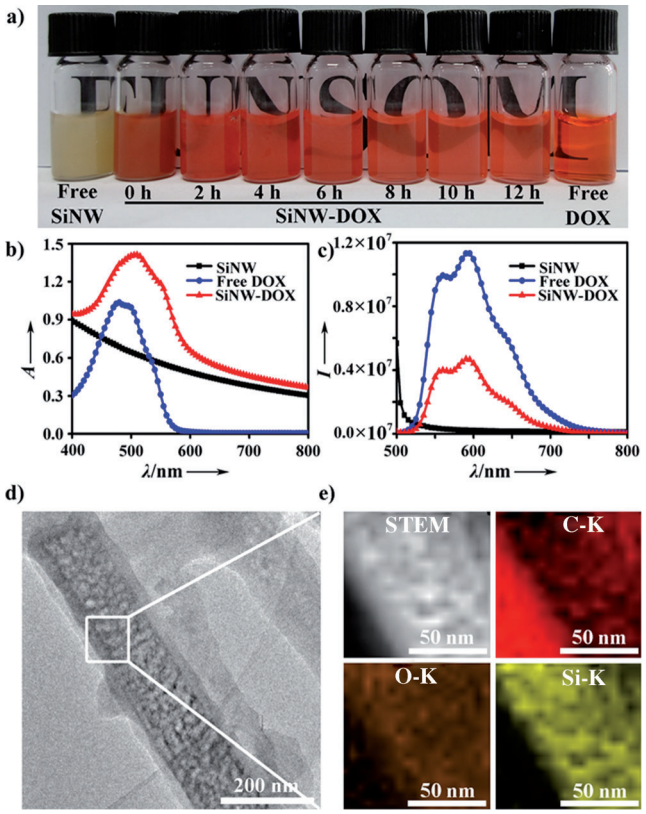

Figure 1. a) Digtial images of SiNWs (left), DOX-loaded SiNWs (reaction time: 0, 2, 4, 6, 8, 10 and 12 h) and free DOX (right). b) Absorption and c) photoluminescence spectra of free DOX, free SiNWs, and the SiNW–DOX complex (loading pH 9). d) A TEM image of the SiNW–DOX complex (loading pH 9). e) Dark-field STEM and corresponding energy-dispersive X-ray (EDX) elemental mapping images of the SiNW–DOX complex in the white frame of (d). For EDX mapping, C, O, and Si element are shown in red, brown, and yellow, respectively.

free DOX molecules remain in the supernatant because of their low molecular weight.[1c,f,g] Afterwards, the precipitate is collected and washed with physiological buffers (PB) for several times until no visible red color is noticeable in the supernatant, indicating the complete removal of residual DOX molecules. UV photoluminescence spectra of the SiNW–DOX complex are shown in Figure 1b and 1c. In comparison to the feeble fluorescence of the pure SiNWs (black line), the SiNW–DOX complex shows distinct and strong absorption and emission peaks at about 490 and 600 nm (red line), respectively, which are ascribed to DOX molecules (blue line) adsorbed on SiNWs. Notably, the fluorescence of DOX is quenched by the SiNWs because of the overlay of the UV/Vis spectrum of the SiNWs with the fluorescence spectrum of DOX, resulting in a relatively low photoluminescence intensity of the SiNW–DOX complex compared to that of free DOX.[4b,8]

As shown in the transmission electronic microscopy (TEM) image (Figure 1d), a DOX layer is obviously observed on the SiNW surface of the SiNW–DOX complex. Moreover, a dark-field scanning TEM (STEM) image further confirms sufficient carbon atoms of DOX on the SiNW–DOX complex (Figure 1e), which is in striking contrast to the pure SiNW without DOX layer in the TEM and STEM images (Figure S2). It is worthwhile to point out that DOX molecules are not released from the SiNW–DOX complex either under high-speed centrifugation (e.g., at 14800 rpm for 15 minutes, Figure S3a) or large-power sonication (e.g., at 40 Hz for 30 minutes, Figure S3b), indicating strong adhesion between DOX and the SiNWs.

The loading behaviors of DOX on SiNWs in acidic-to-basic environments covering a pH range of 5–9 are quantitatively studied. The concentration of DOX is determined by the characteristic DOX absorption peak at about 490 nm through the established standard curve (Figure S4). We find that the amount of DOX bound to SiNWs is pH-dependent, that is, the 490 nm absorption peak and the 600 nm fluorescence of DOX distinctly decrease as the pH value varies from 9 to 5 (Figure S5). The loading factor (defined as DOX/SiNW weight ratio) decreases from about 20.8 to 17.3, 12.4, 1.5, and 0.7 as the pH is reduced from 9 to 8, 7, 6, or 5, respectively (Figure 2a and Figure S6). This trend is caused by the increased hydrophilicity and higher solubility of DOX at

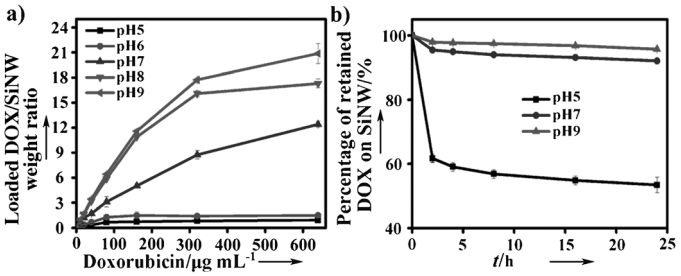

Figure 2. a) Quantification of DOX loading at different pH values (loading pH 5, 6, 7, 8, and 9) with various DOX concentrations. b) DOX retained on SiNWs versus time under pH control (pH 5, 7, and 9).

lower pH because of the enhanced protonation of the -NH_2 group of DOX, and the consequently reduced interaction between DOX and SiNWs. A similar pH-dependent loading property has been reported previously in other kinds of nanomaterials-based nanocarriers (e.g. single-walled carbon nanotubes and mesoporous silica nanoparticles).[1b,h] Moreover, the DOX loading efficiency is investigated for different initial DOX concentrations with respect to the same concentration of the SiNWs (200 $\mu g\,mL^{-1}$). As shown in Figure 2a, the amount of DOX loading on the SiNWs gradually increases with increasing initial DOX concentration in neutral and basic environments (pH 7–9). Of particular significance is that the loading capacity of DOX dramatically increases to 20800 $mg\,g^{-1}$ under optimum conditions (e.g., at pH 9 and a DOX concentration of 640 $\mu g\,mL^{-1}$; see the detailed calculation in the Supporting Information), which is, to the best of our knowledge, the highest value ever reported for any nanocarrier (e.g., the loading capacity of DOX onto the SWNTs is about 4000 $mg\,g^{-1}$ at a similar DOX concentration).[1b] Next we investigate the DOX releasing behavior of the SiNW–DOX complex prepared at pH 9. The concentrations of the released DOX are determined by measuring the absorbance at 490 nm of DOX in the supernatants after centrifuging the mixtures at various time points. Particularly,

DOX molecules stacked on SiNWs remain stable in basic and neutral buffer, that is, about 8.0% or 4.3% DOX is released from SiNWs at pH 7 or 9 in 24 h, respectively. In sharp contrast, as much as 50% of DOX is released from SiNWs in 24 h at pH 5 (Figure 2b), due to protonation and solubility of DOX in acidic environments.[1b] It is worth pointing out that the pH-dependent drug-loading and releasing properties are favorable for cancer therapy, since the microenvironments of extracellular tumors tissues and intracellular lysosomes and endosomes are acidic,[9] facilitating active drug release from the SiNW-based DOX delivery vehicles.

To evaluate the SiNW–DOX complex for in vitro and in vivo cancer therapy, we integrate behaviors of SiNW–DOX internalization and intracellular drug release by using two typical kinds of cancer cell lines, that is, human epithelial cervical cancer cells (Hela cells) and human oral squamous carcinoma cells (KB cells), as models. DOX with red fluorescence are monitored by laser scanning confocal microscopy (LSCM). To investigate the intracellular localization of DOX released from the SiNW–DOX complex, Hela cells are labeled with LysoTracker Green DND-26, which is specialized for lysosome labeling. After 12 h of incubation with Hela cells, free DOX is mostly localized in the nuclei, and a small fraction of DOX is observed in the cytoplasm (Figure 3a). In contrast, the SiNW-DOX complex, which is co-localized with LysoTracker Green, is primarily distributed in cytoplasm and lysosome. DOX molecules are thus efficiently released from the SiNW–DOX complex distributed in lysosome because of its acidic environment (pH 5.0).[1b,c,f–h] As a result, the released DOX is then translocated into the nucleus by proteasome (Figure 3b).[10] The above data suggest that the accumulation of DOX in the nucleus is due to cellular internalization of the SiNW–DOX complex, followed by intracellular drug release and subsequent trafficking of the drug into the nucleus. Consequently, the SiNW–DOX complexes accumulated in the lysosome may enable continual DOX release, ensuring a slower and prolonged DOX accumulation in the nucleus and adequate drug concentration to continually kill cancer cells.[1g] Similar results are observed in KB cells treated with free DOX and DOX-loaded SiNWs (Figure 3c and d).

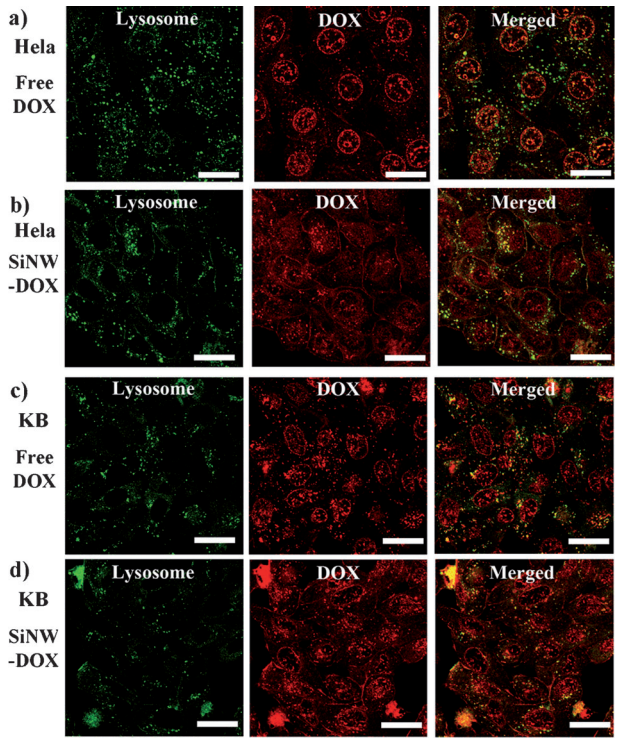

Figure 3. LSCM images of intracellular distribution of free DOX and DOX-loaded SiNWs in Hela (a and b) and KB (c and d) cells. The cells are incubated with free DOX (a and c, 5 μg mL^{-1}) and SiNW–DOX complex (b and d, 5 μg mL^{-1} DOX) for 12 h at 37 °C, followed by treatment with LysoTracker Green DND-26 for 30 minutes. (The LysoTracker or DOX (free DOX, released DOX, and DOX retained on SiNWs) fluorescence is defined as green or red, respectively.)

A consensus has been reached that DOX molecules distributed in nuclei can induce significant cell death.[1b,c,f–h] Thus, we further evaluate the in vitro toxicity of the prepared SiNW–DOX complex. Indeed, the complex results in significant time- and concentration-dependent cell death, similar to that of free DOX (Figure 4). Typically, while the SiNW–DOX complex at low concentrations (e.g., 1.25 μg mL^{-1} DOX) has little influence on the Hela cells, the cell viability is obviously

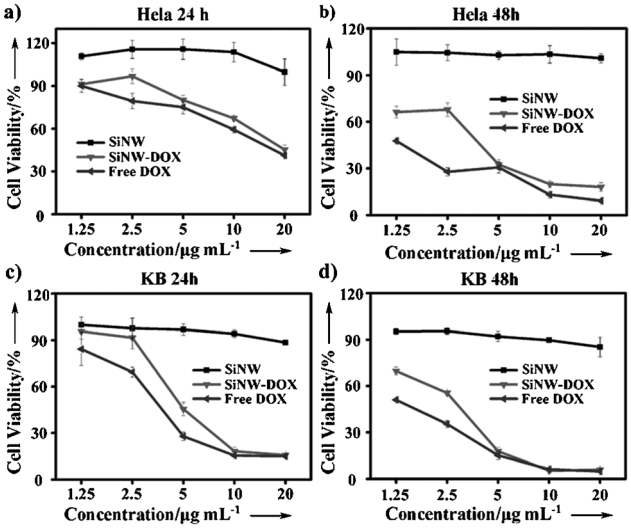

Figure 4. In vitro concentration-dependent cell viability of Hela (a and b) and KB (c and d) cells. The cells are incubated with free SiNWs, SiNW-DOX, and free DOX for 24 (a and c) and 48 h (b and d), as indicated.

reduced to about 40% when cells are incubated with SiNW–DOX complexes of high concentrations (e.g., 20 μg mL^{-1} DOX) for 24 h (Figure 4a), and further decreases to 20% at 48 h of incubation (Figure 4b). A similar tendency is observed for KB cells (Figure 4c and 4d). It is worth noting that, in comparison to severe cytotoxicity of the SiNW-DOX complex, cells incubated with pure SiNWs preserve high cell viability (>90%), suggesting that the SiNWs may serve as noncytotoxic drug nanocarriers because of the favorable biocompatibility of silicon.[3,4]

We further perform in vivo therapeutic examinations on mice bearing KB tumors on their back. Female nude mice with subcutaneous KB xenografts divided into groups are

intratumorally administered with a single dose of physiological saline, pure SiNWs, free DOX, and SiNW–DOX complexes, respectively. For mice injected with DOX or SiNW–DOX complexes, we choose two concentrations of 5 and 25 mg kg^{-1} defined by the DOX concentration. After injection of DOX or the SiNW–DOX complex at 25 mg kg^{-1}, the intratumoral doxorubicin distribution is analyzed by the DOX fluorescence captured by a Maestro EX in vivo fluorescence imaging system. The mouse autofluorescence or DOX fluorescence is defined as white or red by spectral unmixing using the Maestro software. As shown in Figure 5 a, no DOX fluorescence is detected in mice treated by physiological saline or SiNWs; in comparison, distinct DOX red signals are observed in the tumor injected with free DOX or SiNW–DOX. Notably, with prolonged post-injection time, the intensity of the red fluorescence in the tumor region injected with free DOX rapidly drops (about 8 day) and finally diminishes (about 20 day) due to its low penetration ability for tumor tissue.[2] In marked contrast, SiNW–DOX complex-treated mice preserve noticeable DOX accumulation in the tumor region with spectrally resolved red fluorescence even 20 day after injection, which is the longest accumulation time of DOX released from nanomaterials-based drug carriers ever reported under the same experiment conditions (e.g., DOX released from silica- or poly(ethylene glycol)-*b*-polycaprolactone gel-based nanocarriers preserved in the tumor site 7 or 15 days after injection).[1g] We attribute such long-time DOX accumulation to a high drug-loading capacity of SiNWs (20 800 mg g^{-1}), much larger than those of other nanomaterials-based carriers (1200–4000 mg g^{-1}).[1b–d,f–h] Such prolonged SiNW–DOX complexes in the tumor site is favorable for enhancement of the tumor therapy efficiency, since stable and continual release of DOX from SiNW-DOX can effectively kill cancer cells and inhibit tumor growth in long-term treatment.[1g] Quantitative measurement of inhibition of tumor growth, analyzed by monitoring the tumor growth rates in terms of tumor volume changes, further confirms the superior therapeutic efficacy of the SiNW-based nanocarriers. Black and green lines in Figure 5 b display a time-related increase in tumor volume of the two control groups, that is, physiological saline or pure SiNW-administered mice, showing average fractional tumor volumes (V/V_0) of 11.9 ± 3.5 (black line) or 14.6 ± 4.0 (green line), respectively, on day 16. In terms of another control group (e.g., free DOX-treated mice), while tumor growth is inhibited to some extent (blue line), the tumor size inevitably increases, leading to lethality in mice in about 30 day (Figure S10). In striking contrast, the SiNW–DOX group produces remarkable inhibition efficiency of tumor growth, that is, SiNW-DOX-treated mice survive over 30 days without any observed tumor growth (red lines in Figure 5 and Figure S10), which is comparable to the longest inhibition time ever reported for tumor growth using nanomaterials-based drug carriers for cancer therapy.[1g]

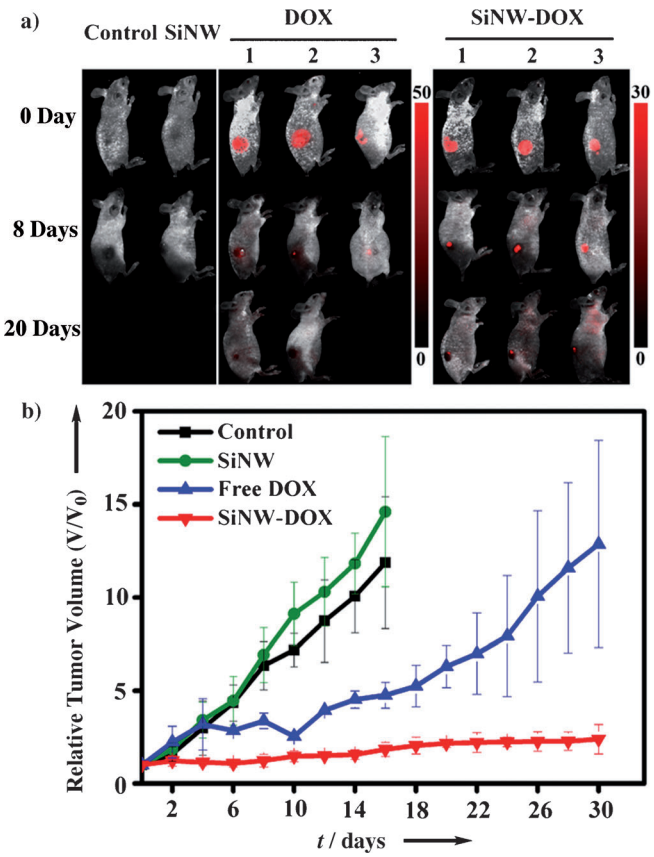

Figure 5. a) Spectrally unmixed in vivo fluorescence images of KB bearing nude Balb/c mice at different time points post intratumoral injection of PBS, free SiNWs, free DOX (25 mg kg^{-1}), and SiNW–DOX (25 mg kg^{-1}). The mouse autofluorescence is defined as white and the DOX fluorescence is defined as red by spectral unmixing in the above images. The intensity of the DOX fluorescence in SiNW-DOX-treated mice is low relative to that of the free DOX-treated group, because of the long-range energy transfer from DOX to SiNWs.[4b,8] b) Tumor growth inhibition at different time points post intratumoral injection of physiological saline, free SiNWs, free DOX (5 mg kg^{-1}), and SiNW–DOX (5 mg kg^{-1}).

In summary, we show that SiNW-based nanocarriers can be used for high-performance intracellular delivery of the antitumor drug DOX. Of particular significance, the SiNW–DOX complex features an extremely large DOX-loading capacity (20 800 mg g^{-1}), which is much higher than those previously reported for nanomaterials-based drug carriers (about 1200–4000 mg g^{-1}). In vitro experiments reveal that the SiNW–DOX complex is mostly accumulated in lysosome, which facilitates continual DOX release and efficient cancer cell destruction. We further demonstrate that DOX-loaded SiNWs are highly efficacious for inhibiting tumor growth in vivo, as SiNW-DOX-treated mice survive over 30 days without obvious detectable tumor growth. Given that SiNWs can be readily produced with high yield and low cost, the SiNWs-based nanocarriers may serve as a practical and powerful tool for cancer therapy, rivalling or complementing the state-of-the-art nanomaterials-based nanocarriers. The present results suggest an exciting potential for SiNW-based nanocarriers as efficient antitumor agents and chemotherapeutic delivery to cellular and molecular targets.

Received: August 20, 2012
Revised: November 26, 2012
Published online: December 11, 2012

Keywords: cancer therapy · drug delivery · nanocarriers · nanowires · silicon

[1] a) S. Giri, B. G. Trewyn, M. P. Stellmaker, V. S. Y. Lin, *Angew. Chem.* **2005**, *117*, 5166 – 5172; *Angew. Chem. Int. Ed.* **2005**, *44*, 5038 – 5044; b) Z. Liu, X. Sun, N. Nakayama-Ratchford, H. Dai, *ACS Nano* **2007**, *1*, 50 – 56; c) X. Y. Yang, X. Y. Zhang, Z. F. Liu, Y. F. Ma, Y. Huang, Y. S. Chen, *J. Phys. Chem. C* **2008**, *112*, 17554 – 17558; d) Z. Liu, J. T. Robinson, X. M. Sun, H. J. Dai, *J. Am. Chem. Soc.* **2008**, *130*, 10876 – 10877; e) Y. N. Zhao, B. G. Trewyn, I. I. Slowing, V. S. Y. Lin, *J. Am. Chem. Soc.* **2009**, *131*, 8398 – 8400; f) Y. Chen, H. R. Chen, L. M. Guo, Q. J. He, F. Chen, J. Zhou, J. W. Feng, J. L. Shi, *ACS Nano* **2010**, *4*, 529 – 539; g) H. P. Rim, K. H. Min, H. J. Lee, S. Y. Jeong, S. C. Lee, *Angew. Chem.* **2011**, *123*, 9015 – 9019; *Angew. Chem. Int. Ed.* **2011**, *50*, 8853 – 8857; h) L. M. Zhang, Z. X. Lu, Q. H. Zhao, J. Huang, H. Shen, Z. J. Zhang, *Small* **2011**, *7*, 460 – 464.

[2] a) A. J. Primeau, A. Rendon, D. Hedley, L. Lilge, I. F. Tannock, *Clin. Cancer Res.* **2005**, *11*, 8782 – 8788; b) A. I. Minchinton, I. F. Tannock, *Nat. Rev. Cancer* **2006**, *6*, 583 – 592.

[3] a) Y. He, Z. H. Kang, Q. S. Li, C. H. A. Tsang, C. H. Fan, S. T. Lee, *Angew. Chem.* **2009**, *121*, 134 – 138; *Angew. Chem. Int. Ed.* **2009**, *48*, 128 – 132; b) Y. He, Y. Y. Su, X. B. Yang, Z. H. Kang, T. T. Xu, R. Q. Zhang, C. H. Fan, S. T. Lee, *J. Am. Chem. Soc.* **2009**, *131*, 4434 – 4438; c) Y. He, Y. L. Zhong, F. Peng, X. P. Wei, Y. Y. Su, Y. M. Lu, S. Su, W. Gu, L. S. Liao, S. T. Lee, *J. Am. Chem. Soc.* **2011**, *133*, 14192 – 14195; d) J. Park, L. Gu, G. Maltzahn, E. Ruoslahti, S. N. Bhatia, M. J. Sailor, *Nat. Mater.* **2009**, *8*, 331 – 336.

[4] a) Y. He, Y. L. Zhong, F. Peng, X. P. Wei, Y. Y. Su, S. Su, W. Gu, L. S. Liao, S. T. Lee, *Angew. Chem.* **2011**, *123*, 3136 – 3139; *Angew. Chem. Int. Ed.* **2011**, *50*, 3080 – 3083; b) S. Su, X. P. Wei, Y. L. Zhong, Y. Y. Guo, Y. Y. Su, Q. Huang, S. T. Lee, C. H. Fan, Y. He, *ACS Nano* **2012**, *6*, 2582 – 2590; c) Y. Y. Su, X. P. Wei, F. Peng, Y. L. Zhong, Y. M. Lu, S. Su, T. T. Xu, S. T. Lee, Y. He, *Nano Lett.* **2012**, *12*, 1845 – 1850.

[5] a) M. W. Shao, L. Cheng, X. H. Zhang, D. D. D. Ma, S. T. Lee, *J. Am. Chem. Soc.* **2009**, *131*, 17738 – 17739; b) Y. Q. Qu, L. Liao, Y. J. Li, H. Zhang, Y. Huang, X. F. Duan, *Nano Lett.* **2009**, *9*, 4539 – 4543; c) A. I. Hochbaum, D. Gargas, Y. J. Hwang, P. D. Yang, *Nano Lett.* **2009**, *9*, 3550 – 3554.

[6] a) K. Q. Peng, A. J. Lu, R. Q. Zhang, S. T. Lee, *Adv. Funct. Mater.* **2008**, *18*, 3026 – 3035; b) Y. He, C. H. Fan, S. T. Lee, *Nano Today* **2010**, *5*, 282 – 295; c) Y. He, S. Su, T. T. Xu, Y. L. Zhong, J. A. Zapien, J. Li, C. H. Fan, S. T. Lee, *Nano Today* **2011**, *6*, 122 – 130; d) Y. L. Zhong, F. Peng, X. P. Wei, Y. F. Zhou, J. Wang, X. X. Jiang, Y. Y. Su, S. Su, S. T. Lee, Y. He, *Angew. Chem.* **2012**, *124*, 8613 – 8617; *Angew. Chem. Int. Ed.* **2012**, *51*, 8485 – 8489.

[7] a) M. Vallet-Regí, F. Balas, D. Arcos, *Angew. Chem.* **2007**, *119*, 7692 – 7703; *Angew. Chem. Int. Ed.* **2007**, *46*, 7548 – 7558; b) G. A. Hughes, *Nanomedicine* **2005**, *1*, 22 – 30.

[8] a) D. J. Maxwell, J. R. Taylor, S. M. Nie, *J. Am. Chem. Soc.* **2002**, *124*, 9606 – 9612; b) R. H. Yang, J. Y. Jin, Y. Chen, N. Shao, H. Z. Kang, Z. Y. Xiao, Z. W. Tang, Y. R. Wu, Z. Zhu, W. H. Tan, *J. Am. Chem. Soc.* **2008**, *130*, 8351 – 8358; c) S. P. Song, Z. Q. Liang, J. Zhang, L. H. Wang, G. X. Li, C. H. Fan, *Angew. Chem.* **2009**, *121*, 8826 – 8830; *Angew. Chem. Int. Ed.* **2009**, *48*, 8670 – 8674.

[9] a) I. F. Tannock, D. Rotin, *Cancer Res.* **1989**, *49*, 4373 – 4384; b) N. Raghunand, R. A. Gatenby, R. J. Gillies, *Br. J. Radiol.* **2003**, *76*, S11 – S22; c) R. A. Gatenby, R. J. Gillies, *Nat. Rev. Cancer* **2004**, *4*, 891 – 899.

[10] K. Kiyomiya, S. Matsuo, M. Kurebe, *Life Sci.* **1998**, *62*, 1853 – 1860.

